Kinetics of the Reaction of CO_2/CO Gas Mixtures with Iron Oxide

ELIZABETH J. WORRAL and KENNETH S. COLEY

The kinetics of the oxygen exchange reaction between carbon dioxide and carbon monoxide were measured on iron, wüstite, and magnetite surfaces. This was done through the use of an isotope exchange technique. The measured rate constants are dependent on the oxygen activity. This dependence is expressed by $k_a = k_o a_O^{-m}$. The parameter m was found to have values between 0 and 1. It was found that, in the iron region, the apparent rate constant was independent of the oxygen partial pressure (*i.e.*, $m = 0$) at 1123 K (850 °C) and that it was inversely dependent on the oxygen partial pressure (*i.e.*, $m = 1$) for the magnetite region at 1123 K (850 °C) and 1268 K (995 °C). In the wüstite region, m was found to be equal to 0.51, 0.66, and 1.0 for the w_1, w_2, and w_3 pseudo phases, respectively, at 1268 K (995 °C). At 1123 K (850 °C), in wüstite, m was found to be equal to 0.59 and to 1.0 for the w_1' and w_3' pseudo phases, respectively.

DOI: 10.1007/s11663-010-9358-4

I. INTRODUCTION

THE kinetics of oxygen exchange between gases and metal or oxide substrates is important in understanding oxidation and reduction. Even when diffusion in the solid controls the overall rate, the relative kinetics of competing reactions can have a strong influence on the local thermodynamic conditions and can control which phase will form.[1–7] As part of an overall study on the role of competition between reactions of different gases at solid surfaces, the authors investigated the kinetics of oxygen exchange on the surface of iron and iron oxides.

A. *Kinetics of Oxygen Exchange on Iron Oxide*

In previous research on oxygen exchange between CO_2 and iron oxide, Grabke and Viefhaus[8] found the oxygen activity dependence of the apparent rate constant, k_a, to follow Eq. [1] with a constant value of m, which is expressed as follows:

$$k_a = k_o a_O^{-m}. \quad [1]$$

Grabke[9,10] proposed a mechanism for the reaction based on electron transfer to an adsorbed CO_2 molecule. These workers claimed the oxygen activity dependence resulted from the electron defect structure of the oxide. However, it is now known that the defect structure of wüstite is much more complex than assumed by Grabke. The complexity of the defect structure is such that some workers have proposed several pseudo phases to exist within the wüstite phase field. The existence of pseudo phases remains controversial, but the complexity of the defect structure and the fact that it changes with oxygen potential is now well established. It should be expected that such a complex defect structure would lead to a more complex relationship than that defined by Eq. [1].

B. *Pseudo Phases of Iron Oxide*

The existence of pseudo phases in the wüstite phase field has been the subject of much debate. Vallet *et al.*[11] were the first to suggest that the wüstite phase was more complex than originally thought. Since the initial work by Vallet *et al.*, the wüstite phase field has been probed by many methods to determine whether the pseudo phases exist. Evidence for their existence has been provided by dilatometry,[12–14] X-ray diffraction,[12,13,15,16] thermogravimetry,[17–25] neutron diffraction,[26] electromotive force,[27,28] and electrical conductivity[29,30] measurements. However, various studies have been conducted that have provided no evidence for the existence of more than one phase in wüstite. These studies include those which provide thermogravimetetric,[31] electromotive force,[32–34] X-ray diffraction,[35] and work function[36] measurements.

C. *Effect of Defect Structure on Kinetics of Interfacial Reactions*

In studies using the isotope exchange technique, the gases are in equilibrium with the condensed phase, but the isotopes of these gases are not in equilibrium. In this situation, the kinetics of the reaction can be determined when the system is at chemical equilibrium. The resulting data can be used to determine the rates at which surface reactions take place and the reactions that will dominate nonequilibrium systems. In using this

ELIZABETH J. WORRAL, Metallurgist, is with Severstal Dearborn, 14661 Rotunda Drive, Dearborn, MI 48120. Contact e-mail: eworral@severstalna.com KENNETH S. COLEY, Professor, is with the Department of Materials Science and Engineering, McMaster University, 1280 Main Street West, Hamilton, Ontario L8S 4L7, Canada.

Manuscript submitted May 1, 2006.
Article published online April 15, 2010.

method to study corrosion, the influence of solid-state diffusion control is eliminated, and so, the surface reaction rates can be determined.

This technique has been employed for studying metallurgical reactions at high temperatures by Grabke, Belton, and Sano and their associates in order to investigate the water–gas shift reaction on metal[37] and on FeO[9,38] surfaces. This method also has been used to look at the rate of oxygen transfer reactions at high temperatures on metal surfaces,[39–41] oxides,[10] liquid metals,[42,43] and liquid slags.[5,44–47]

Both Grabke and Belton explored the kinetics of oxygen transfer in high-temperature reactions on many surfaces using an isotope exchange reaction. The overall reaction in these studies is given by Eq. [2] in which * indicates a labeled isotope (*i.e.*, either carbon 13 or 14).

$$^{*}CO_2 + CO \rightleftarrows {}^{*}CO + CO_2 \qquad [2]$$

This reaction can be broken down into the following two partial reactions:

$$^{*}CO_2 \rightleftarrows {}^{*}CO + O_{(ads)} \qquad [3]$$

$$CO + O_{(ads)} \rightleftarrows CO_2 \qquad [4]$$

The rate constant determined from isotope exchange experiments is not necessarily a true rate constant. It has been determined to be proportional to the carbon dioxide partial pressure as well as dependent on the ratio of CO_2/CO in the gas and the oxygen activity on the oxide surface. In keeping with convention, the authors have termed this measured rate constant the apparent rate constant. The apparent rate constant therefore was determined to be equated to a true rate constant multiplied by the oxygen activity to some power. This can be seen in Eq. [1] where k_a is the apparent rate constant, k_o is the true rate constant (dependent on temperature only), a_O is the oxygen activity, and m is a value between 0 and 1. The dependence on the oxygen activity given by m has been stated by Grabke and Viefhaus[8] to be influenced by the degree of coverage with adsorbed oxygen or by the electronic or ionic disorder of the oxide. However, Grabke and Viefhaus also have shown that there is little preferential adsorption of oxygen at temperatures above 1073 K (800 °C).

The electronic or ionic disorder of the oxide also can have an effect on m. For a simple defect structure involving randomly distributed cation vacancies, the concentration of electron holes is proportional to the oxygen activity to the 1/2 or to the 1/3 for singly and doubly charged metal vacancies, respectively. Taking into account the surface reaction (*i.e.*, the decomposition of carbon dioxide) it is seen that an electron transfer to the oxygen atom must take place. This transfer can occur during the adsorption step (Eq. [5]), in the dissociation step to the activated complex (Eq. [6]), or to the adsorbed oxygen after the reaction (Eq. [7]).[9]

$$CO_{2(g)} \rightleftarrows CO^{\delta-}_{2(ads)} \rightleftarrows {}^{\dagger}CO^{\delta-}_{2(ads)} \rightleftarrows CO_{(g)} + O^{\delta-}_{(ads)} \qquad [5]$$

$$CO_{2(g)} \rightleftarrows CO_{2(ads)} \rightleftarrows {}^{\dagger}CO^{\delta-}_{2(ads)} \rightleftarrows CO_{(g)} + O^{\delta-}_{(ads)} \qquad [6]$$

$$CO_{2(g)} \rightleftarrows CO_{2(ads)} \rightleftarrows {}^{\dagger}CO_{2(ads)} \rightleftarrows CO_{(g)} + O^{\delta-}_{(ads)} \qquad [7]$$

In these equations, δ is the number of transferred electrons and can be equal to 1 or 2. If the electron transfer to the oxygen occurs after the reaction to form adsorbed oxygen (Eq. [7]), then the reaction rate is not dependent on the electronic properties of the oxide. If the electron transfer is from either mechanism in Eqs. [5] or [6], then the reaction rate may be dependent on the oxide electronic properties, provided the adsorption step is not rate controlling. The surface concentration for the adsorbed charged carbon dioxide molecule is given by Eq. [8] for Eq. [5] and by Eq. [9] for Eq. [6], for p-type reactions as follows:

$$CO_{2(g)} \rightleftarrows CO^{\delta-}_{2(ads)} + \delta h^{\bullet} \qquad [8]$$

$$CO_{2(ads)} \rightleftarrows {}^{\dagger}CO^{\delta-}_{2(ads)} + \delta h^{\bullet} \qquad [9]$$

From this, it can be seen that the surface concentration of $CO^{\delta-}_{2(ads)}$ or ${}^{\dagger}CO^{\delta-}_{2(ads)}$ molecules is inversely proportional to the concentration of holes and to the number of transferred electrons. Taking into account both the defect structure of the oxide and the electron transfer in the surface reaction for Eqs. [8] and [9], the dependence on the oxygen activity can be determined. The surface concentration of the adsorbed charged carbon dioxide molecule is proportional to $a_O^{-\delta/2}$ or $a_O^{-\delta/3}$ for singly and doubly charged metal vacancies, respectively.

Taking into account both the degree of coverage with adsorbed oxygen and the electronic or ionic disorder of the oxide, Eq. [1] can be rewritten as Eq. [10] for doubly charged metal vacancies.[8] The dependence on the oxygen activity m then equals $\gamma + \delta/3$, in which γ is the exponent for the adsorbed oxygen effect and $\delta/3$ is the exponent for the effect of the electron transfer. A similar equation can be written for singly charged metal vacancies. It should be noted that, in the present work, γ can be assumed to equal to 0 because adsorbed oxygen was shown to have a negligible effect by Grabke and Viefhaus.[8] Equation 10 is expressed as follows:

$$k_a = k_o a_O^{-\gamma} a_O^{-\delta/3} p_{CO_2} \qquad [10]$$

Grabke[10] conducted experiments on wüstite and magnetite and the experimental values of m were determined, which can be seen in Table I. Table I also shows the results obtained by Meschter and Grabke[38] on wüstite as well as the expected values for the participation of one or two electrons in the surface reaction. As suggested previously, it seems unlikely that m will have a constant experimental value throughout the wüstite phase field, as the concentration of electron holes is known to have a complex dependency on oxygen activity.

Table I. Experimental Values of m for Wüstite and Magnetite and Expected m Values for the Participation of One or Two Electrons (δ Equaling 1 or 2)[9]. A – Grabke,[10] and B – Meschter and Grabke[38]

Oxide	Temperature (K (°C))	m (Expected Value) $\delta = 1$	m (Expected Value) $\delta = 2$	m (Experimental) A	m (Experimental) B
$Fe_{1-x}O$	1073 (800)	1/3	2/3	1	0.52
	1173 (900)	1/3	2/3	0.7	0.68
	1256 (983)	1/3	2/3	0.6	
	1273 (1000)	1/3	2/3		0.59
Fe_3O_4	1073 (800)	0	0	0.5	
	1173 (900)	0	0	0.5	
	1256 (983)	0	0	0.5	

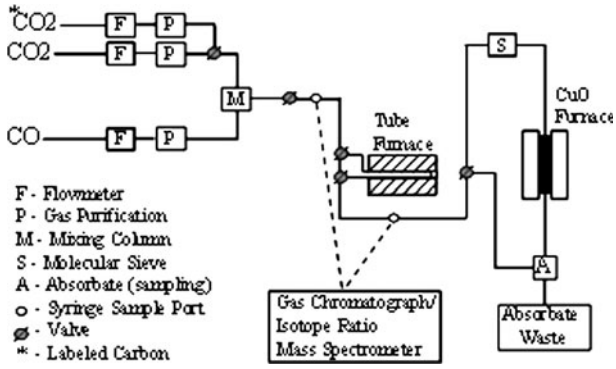

Fig. 1—A schematic of the experimental apparatus for the isotope exchange experiments.

II. EXPERIMENTAL PROCEDURE

The surface reaction rates were measured using an isotope exchange reaction in which a setup similar to that employed in previous studies by Grabke and Belton[5,9,10,37–46] was used. A schematic of the apparatus can be seen in Figure 1, and a diagram of the sample arrangement is shown in Figure 2.

The experiments conducted involved flowing carbon dioxide and carbon monoxide gases, of varying ratios, over iron and iron oxides at various temperatures. The carbon dioxide portion of the gas consisted of both labeled and unlabeled carbon. The labeled carbon was tracked throughout the reaction by analyzing the ingoing and outgoing gases.

The flow rates of the gases, as they exited the gas cylinders, were regulated by electronic mass flow controllers. Each of the gases present in the experiment passed through separate drying columns. The drying columns were 42 cm in length and 3 cm in diameter and contained equal amounts of first, silica gel and then, Drierite (anhydrous calcium sulfate). The carbon monoxide gas then went though a similar size column containing Lecosorb (Leco, St. Joseph, MI) indicator pellets to clean the gas of any carbon dioxide. Lecosorb consists of sodium hydroxide on a nonfibrous silicate carrier. Once all gases had been dried and cleaned, they were mixed in a column containing glass beads. The resulting gas stream then was directed to the tube furnace that contained the metal sample. The gas stream was jetted continuously onto the sample for the duration of the experiment.

Unlabeled carbon dioxide and carbon monoxide gases in the desired ratio and flow rates were passed over the sample until the desired temperature was reached and for several hours thereafter to establish equilibrium. The labeled carbon dioxide then was introduced into the stream, and the unlabeled carbon dioxide was adjusted so that the CO_2/CO ratio remained constant, and samples then were taken. Multiple samples were taken to ensure that the system had reached steady-state conditions. Once a steady state condition had been reached, the CO_2/CO ratio,

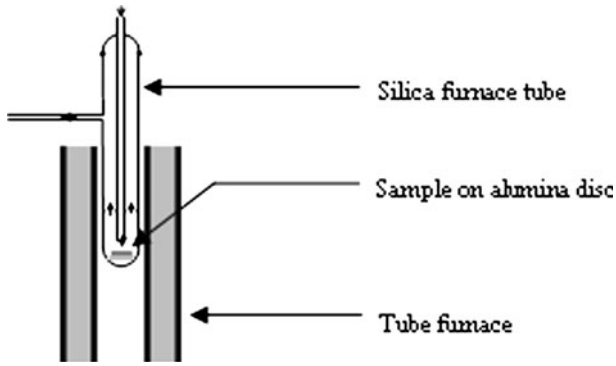

Fig. 2—A diagram of the sample arrangement. Small arrows show the direction of the gas flow.

temperature, or flow rate could be changed, and another experiment conducted.

Iron foil samples, 99.5 pct pure, < 0.05 pct S, supplied by Goodfellow Corporation (Oakdale, PA), were cut to approximately 2.5 cm $\times$ 2.5 cm and cleaned with acetone. Samples then were placed in the furnace and exposed to the experimental atmosphere in the manner described. In most cases, the conditions resulted in oxide formation on the surface. To check the effect of the oxidation procedure on the measurements, repeat experiments were conducted in which the sequence of oxidation was changed. An example of one sequence is as follows: the metal was oxidized to form wüstite, and after equilibration, a measurement was taken; the oxygen potential then was increased and another measurement taken, and this process was repeated several times. In other cases, the process would start with the most oxidizing condition, and increasingly, more reducing conditions would be employed in subsequent measurements. In other cases, a random change in oxidizing condition was employed. In all these cases, the measurements at a particular condition were the same within experimental error. The only exception to this was when a sample was oxidized and subsequently reduced across a phase boundary—wüstite to iron or magnetite to wüstite. In these cases, there was considerable scatter in

the data, which was ascribed to differences in the surface area caused by reduction. All data obtained this way was discarded.

Samples of iron and oxidized iron were taken for X-ray diffraction and scanning electron microscopy to verify that the phase being investigated actually was produced. That is, for the iron samples, that no oxide was formed, and for FeO and Fe_3O_4 samples, that the oxide had formed and completely covered the metal surface. Metal samples showed no visual discoloration, and oxide samples were fine grained and essentially featureless.

A. *Carbon-14 Experiments*

For the carbon-14 analysis, the ingoing carbon dioxide and the outgoing carbon monoxide were analyzed. To analyze the outgoing gas, the carbon monoxide had to be separated from the carbon dioxide, and then the carbon monoxide had to be converted to carbon dioxide. Therefore, on leaving the tube furnace, the gas stream was passed through two molecular sieve columns (approximately 220 grams) and one column containing Lecosorb. This process stripped the carbon dioxide from the gas stream. After this was done, the gas was oxidized in a furnace containing approximately 100 grams of CuO to produce carbon dioxide. The oxidized carbon monoxide then was bubbled through 4 ml of a carbon dioxide absorber—a 0.33M NaOH solution—using a coarse fritt. The waste gas then was passed through two columns of molecular sieve and one of Lecosorb. The 4-ml sample was removed from the apparatus when the indicator, phenolpthalein, changed from pink to clear. This indicator was employed to ensure that the same concentration of carbon dioxide was absorbed for each experiment.

In preparing the experiment, the molecular sieves first had to be conditioned to extract any water, carbon dioxide, and other impurities. This extraction was done by increasing the temperature to 823 K (550 °C) for 24 hours while passing argon at a rate of 150 ml per minute through the columns.[48] To achieve the necessary temperature, heating tapes were used, and insulation was wrapped around the columns and the heating tapes. When the column of Lecosorb started to turn white, the carbon dioxide was getting through the molecular sieve without getting trapped, indicating that saturation with carbon dioxide had occurred. For regeneration to occur, the molecular sieves had to be heated to a temperature of 698 K (425 °C) for 5 minutes.[48]

The samples obtained from the ingoing gas and from the outgoing oxidized carbon monoxide gas then were analyzed. To prepare the samples for counting, 1 ml of a sample was pipetted into 10 ml of a scintillation cocktail. A Beckman 6000 series liquid scintillation counter (Beckman Coulter, Brea, CA) was used to determine the counts per minute (cpm). The samples were left in the counter overnight before any measurements were taken to avoid any counts resulting from photoluminescence. Each sample was counted for 2 minutes before the final reading was obtained. These count rates then were used to obtain the apparent rate constant, k_a, via Eq. [11], which is expressed as follows[39]:

$$k_a = \frac{\dot{V}}{ART}\left(\frac{1}{1+B}\right)\ln\left(\frac{1}{1-(N(1+B)/N'B)}\right) \quad [11]$$

where $\dot{V}$ is the volume flow rate, T is the temperature, A is the sample surface area, B is P_{CO_2}/p_{CO}, N' is the counting rate of initial CO_2, and N is the counting rate of CO_2 resulting from conversion of CO.

B. *Carbon-13 Experiments*

For the experiments employing carbon 13 as the labeled species, an isotope ratio mass spectrometer (IRMS) was used to analyze the gas samples. From Figure 1, it can be seen that there were two sampling ports in the experimental apparatus, one before the furnace and one after the furnace. Syringe samples of the gas were taken at these points and then injected into a gas chromatograph/IRMS system. The gas chromatograph separated the carbon dioxide and the carbon monoxide so that the two gases went into the IRMS at different times, and the IRMS was set up to analyze the carbon dioxide gas. The values obtained from the IRMS were, in the case of CO_2, the ratios of mass 45 ($^{13}CO_2$, $C^{17}OO$) to mass 44 (CO_2) were termed the $(2/1)^{CO_2}$ ratio, and mass 46 ($^{14}CO_2$, $C^{18}OO$, $^{13}C^{17}OO$) to mass 44 were termed the $(3/1)^{CO_2}$ ratio. The same terminology is used for CO, except the superscript is CO.

The equation for the calculation of the apparent rate constants using carbon 13 as the labeled species is more complicated than when carbon 14 is used. This is because the natural abundance of the isotope is not negligible and so cannot be ignored in the carbon monoxide gas as was done when the carbon 14 was the labeled isotope. The following is the development of the equation used to obtain the apparent rate constants and the formulae needed to use the information given by the IRMS. The overall reaction is given by Eq. [12], which can be broken down into the two partial reactions, given by Eqs. [13] and [14]. The experiments conducted dealt with the first of the two partial reactions, as the ingoing gases were carbon monoxide as well as labeled and unlabeled carbon dioxide. Equation [15] gives the rate of this reaction. The equations are as follows:

$$^{13}CO_2 + CO \rightleftarrows {}^{13}CO + CO_2 \quad [12]$$

$$^{13}CO_2 \rightleftarrows {}^{13}CO + O_{(ads)} \quad [13]$$

$$CO + O_{(ads)} \rightleftarrows CO_2 \quad [14]$$

$$R = \frac{1}{A}\frac{d\left(n_{13_{CO}} - n^{\circ}_{13_{CO}}\right)}{dt} = k' p_{13_{CO_2}}(1 - \Sigma_i \theta_i) - k'' p_{13_{CO}} \theta_o \quad [15]$$

where k' is the forward rate constant, k'' is the reverse rate constant, θ_i is the fractional coverage's by adsorbed

species I, θ_o is the fractional coverage by oxygen, $n_{13_{CO}}$ is the number of moles of labeled carbon monoxide in the outgoing gas, $n^{\circ}_{13_{CO}}$ is the number of moles of labeled carbon monoxide in the ingoing gas, and p is the partial pressure.

The number of moles then can be converted into partial pressures to give Eq. [16], which is expressed as follows:

$$\frac{V}{ART}\frac{d\left(p_{13_{CO}} - p^{\circ}_{13_{CO}}\right)}{dt} = k' p_{13_{CO_2}}(1 - \Sigma_i \theta_i) - k'' p_{13_{CO}} \theta_o \quad [16]$$

where V is the volume of gas, T is the temperature, and A = is the sample surface area.

The initial partial pressure of the labeled carbon monoxide is a constant value and can be eliminated from the derivative in Eq. [16]. Then, by considering that for isotope exchange equilibrium, Eq. [17] is true, the reverse rate constant can be eliminated to obtain Eq. [18]. Equations [17] and [18] are expressed as follows:

$$\frac{k'' \theta_o}{k'(1 - \Sigma_i \theta_i)} = \frac{p_{CO_2}}{p_{CO}} = \left(\frac{p_{13_{CO_2}}}{p_{13_{CO}}}\right)_{eq} = B \quad [17]$$

$$\frac{V}{ART}\frac{dp_{13_{CO}}}{dt} = k'(1 - \Sigma_i \theta_i)\left(p_{13_{CO_2}} - p_{13_{CO}}\left(\frac{p_{13_{CO_2}}}{p_{13_{CO}}}\right)_{eq}\right) \quad [18]$$

Equation [18] then can be rearranged and integrated to get Eq. [19],[49,50] in which k_a is the apparent rate constant for the reaction and $\dot{V}$ is the volume flow rate of the gas and is expressed as follows:

$$k_a = k'(1 - \Sigma_i \theta_i) = \frac{\dot{V}}{ART}\frac{1}{(1+B)} \ln\left(\frac{1 - p^{\circ}_{13_{CO}}/(p_{13_{CO}})_{eq}}{1 - p_{13_{CO}}/(p_{13_{CO}})_{eq}}\right) \quad [19]$$

From Eq. [19], it can be seen that the terms for the partial pressure of the labeled carbon monoxide of the ingoing ($p^{\circ}_{13_{CO}}$), outgoing ($p_{13_{CO}}$), and equilibrium $\left((p_{13_{CO}})_{eq}\right)$ gases need to be determined. These are given by Eqs. [20] through [22], which are in terms of data that can be obtained from the IRMS and are as follows:

$$p^{\circ}_{13_{CO}} = \frac{(2/1)^{\circ CO}}{(1+B)(1+(2/1)^{\circ CO})} \quad [20]$$

$$p_{13_{CO}} = \frac{1}{(B+1)}\left[\left(\frac{B(2/1)^{\circ CO_2}}{1+(2/1)^{\circ CO_2}}\right) + \left(\frac{(2/1)^{\circ CO}}{1+(2/1)^{\circ CO}}\right) - \left(\frac{B(2/1)^{\circ CO_2}}{1+(2/1)^{\circ CO_2}}\right)\right] \quad [21]$$

$$p^{eq}_{13_{CO}} = \frac{1}{(1+B)^2}\left[\left(\frac{B(2/1)^{\circ CO_2}}{1+(2/1)^{\circ CO_2}}\right) + \left(\frac{(2/1)^{\circ CO}}{1+(2/1)^{\circ CO}}\right)\right] \quad [22]$$

Equations [20] through [22] then were evaluated to get the ingoing, outgoing, and equilibrium partial pressures of the labeled carbon monoxide gas. These values then were substituted into Eq. [19] to get the apparent rate constants for the surface reaction (*i.e.*, the dissociation of carbon dioxide) on the various surfaces considered.

C. *Sources of Error*

The main sources of error in determining the apparent rate constant were measurement and control of flow rate as well as the determination of the concentration of labeled isotopes in ingoing and outgoing gases. In the case of carbon-14 experiments, typical values of N and N' were 3500 to 19,200 and 350,000 to 940,000, respectively. The error for N' was negligible but that for N was 1 pct based on repeat measurements during the same experiment. In the case of carbon-13 experiments, the primary measurement is the ratio of carbon 13 to carbon 12 relative to the same measurement in a standard reference gas. The precision of this measurement is 0.05 pct. The way in which error in flow rate was assessed was changed during this study. Flow rates were measured and found to be precise to 2 pct. When this value is used, propagation of errors gives us an error in k_a of 15 pct to 20 pct for carbon 13 and about twice that for carbon 14. However, repeat experiments under the same conditions suggest an error substantially greater for carbon 14 experiments. As can be seen from Figure 4, this is particularly significant at low pO_2 values. This discrepancy can be understood if we take into account the drift in the electronic flow controllers with temperature on a given day. Periodic calibration of the flow controllers showed very stable behavior. However, later in the study it became clear that significant fluctuations occurred from changes in lab temperature. Consequently, in the later part of the study, flow controllers were calibrated immediately before each experiment, and a spot check was conducted at the end. In this way, it was possible to maintain a precision in the measured k_a for carbon 13 measurements of 15 pct to 20 pct. However the data for carbon14 were obtained early in the study and have built-in errors that limit the conclusions that can be drawn from the data. As far as the errors in the slopes determined for various plots in this study is concerned, these were determined by standard linear regression techniques and are included with the appropriate equation. Blank measurements were done with no sample, and the exchange was considered to be negligible in relation to the measurements on iron and iron oxide.

III. RESULTS

Initial experiments were conducted to determine the range of gas velocities that were acceptable. In isotope

exchange studies there are two following limitations on flow rate: (1) the flow must be sufficiently fast to eliminate gas phase mass transfer control, and (2) the flow must be sufficiently slow to ensure a change in labeled species that can be measured with acceptable precision. This was done by varying the volume flow rate $\left(\dot{V}\right)$ of the gas at a given oxygen partial pressure. These experiments were conducted at 1268 K (995 °C) using CO_2/CO ratios of 1.13 and 0.56 and flow rates of 100 ml/min to 225 ml/min. It was concluded from these experiments that for the entire range of flow rates used, the reaction was in the chemical control regime, as the flow rate did not affect the rate of the reaction. Therefore, only the second limitation was an issue in this case, and for future experiments, flow rates were chosen to be as low as possible while still allowing accurate control of the flow meters.

Experiments were undertaken to determine the temperature dependence of the rate constants at various CO_2/CO ratios and a graph of the results can be seen in Figure 3. The equations of the three lines are given by Eqs. [23] through [25] for CO_2/CO ratios of 0.61, 1.13, and 2.42 respectively, which are as follows:

$$\ln(k_a) = \frac{-23,100}{T} + 1.97 \quad [23]$$

$$\ln(k_a) = \frac{-21,700}{T} + .54 \quad [24]$$

$$\ln(k_a) = \frac{-23,100}{T} + 1.00 \quad [25]$$

where k_a is the apparent rate constant ($mole.cm^{-2}.sec^{-1}.atm^{-1}$). The activation energies calculated from Eqs. [23] through [25] are 192 ± 3 kJ/mol, 180 ± 14 kJ/mol, and 192 ± 5 kJ/mol, respectively.

Experiments also were conducted to determine the dependence of the apparent rate constant on the oxygen partial pressure at temperatures of 1123 K (850 °C) and 1268 K (995 °C). These experiments were done using CO_2/CO ratios (0.15 to 6.5) that allowed the experiments to be carried out in the iron, wüstite, and magnetite phase fields. Results were obtained using both carbon 13 and carbon 14.

The results at 1268 K (995 °C) using carbon 14, with CO_2/CO ratios ranging from 0.578 to 6.5, can be seen in Figure 4. The error bars in this figure represent the standard deviation of the data, and these errors are typical for all of data obtained in this study. In the wüstite phase field, the data is represented by two vertical dashed lines. The line closest to the iron–wüstite boundary is given by Eq. [26] and the one closest to the wüstite–magnetite boundary is given by Eq. [27]. Equation [28] represents the line in the magnetite phase field. It also should be noted that, in the current work, the data in the low oxygen potential region of Figure 4 is relatively scattered. Equations [26] through [28] are depicted as follows:

$$\mathrm{Log}(k_a) = -0.14(\pm 0.10)\mathrm{Log}\left(\frac{CO_2}{CO}\right) - 7.23(\pm 0.02) \quad [26]$$

$$\mathrm{Log}(k_a) = -0.99(\pm 0.06)\mathrm{Log}\left(\frac{CO_2}{CO}\right) - 7.10(\pm 0.03) \quad [27]$$

$$\mathrm{Log}(k_a) = -0.89(\pm 0.13)\mathrm{Log}\left(\frac{CO_2}{CO}\right) - 7.01(\pm 0.10) \quad [28]$$

At 1123 K (850 °C), the exchange reaction on iron was found to be independent of the oxygen partial pressure, and the apparent rate constant that was found is given by Eq. [29], which is expressed as follows:

$$\mathrm{Log}(k_a) = -0.04(\pm 0.49)\mathrm{Log}\left(\frac{CO_2}{CO}\right) - 6.93(\pm 0.22) \quad [29]$$

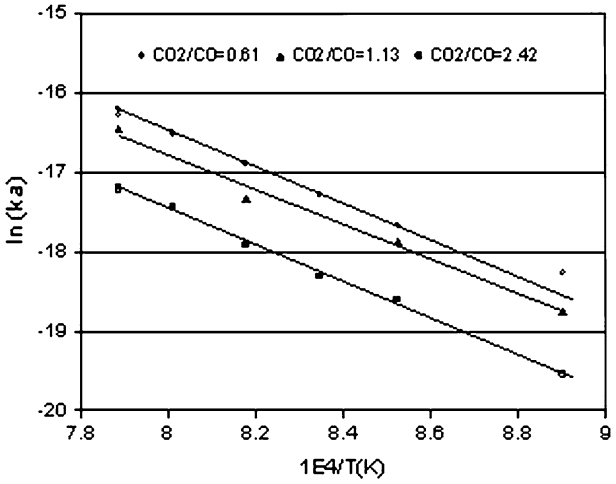

Fig. 3—The temperature dependence of apparent rate constants for various CO_2/CO ratios in the wüstite phase field. Open data points are for extrapolated values.

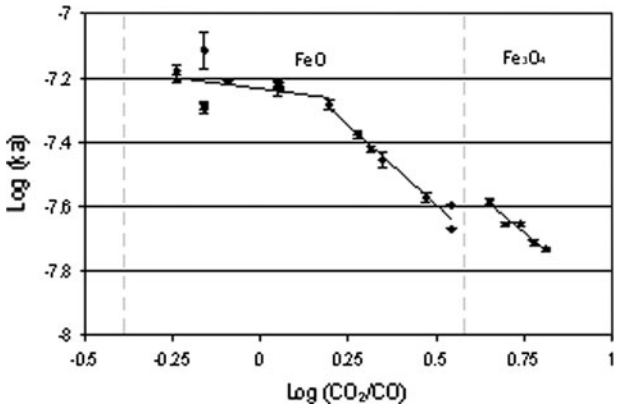

Fig. 4—The effect of the oxygen partial pressure on the rate constant in the wüstite and magnetite regions at 1268 K (995 °C) using carbon 14. The dashed lines represent the phase boundaries.

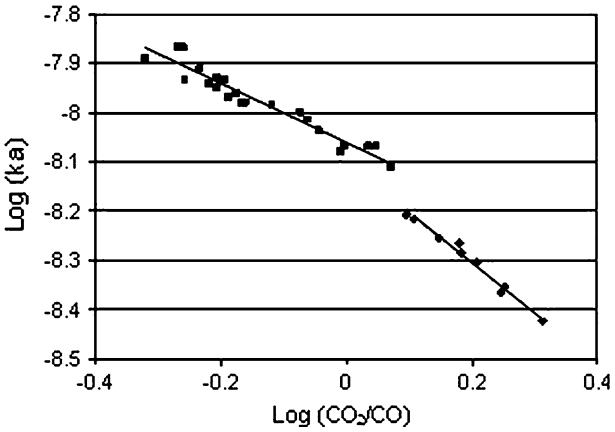

Fig. 5—The effect of the oxygen partial pressure on the apparent rate constant at 1123 K (850 °C) in the wüstite phase field (carbon 13).

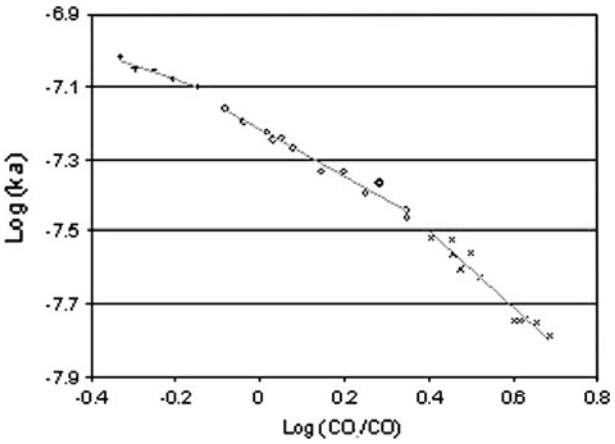

Fig. 6—The effect of the oxygen partial pressure on the apparent rate constant at 1268 K (995 °C) in the wüstite phase field (carbon 13).

In the wüstite region, one straight line did not fit the data accurately. At 1123 K (850 °C) two straight lines could be used to represent the data as is shown in Figure 5, and at 1268 K (995 °C) three straight lines were used, which can be seen in Figure 6.

Experiments also were conducted in the magnetite phase field at 1123 K (850 °C) and 1268 K (995 °C). Figure 7 shows the results for this phase field. The data at 1123 K (850 °C) is given by Eq. [30] and at 1268 K (995 °C) is given by Eq. [31], which are as follows:

$$\mathrm{Log}\,(k_a) = -1.04(\pm 0.07)\mathrm{Log}\left(\frac{CO_2}{CO}\right) - 7.83(\pm 0.04) \quad [30]$$

$$\mathrm{Log}\,(k_a) = -1.03(\pm 0.07)\mathrm{Log}\left(\frac{CO_2}{CO}\right) - 6.86(\pm 0.05) \quad [31]$$

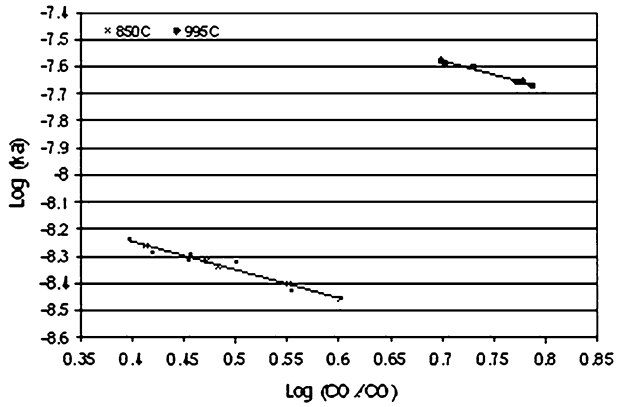

Fig. 7—The effect of the oxygen partial pressure on the apparent rate constant at 1123 K (850 °C) and 1268 K (995 °C) in the magnetite phase field (carbon 13).

IV. DISCUSSION

A. *Activation Energy*

It was shown earlier that the activation energies in the wüstite phase field were equal to 192 ± 3 kJ/mol, 180 ± 14 kJ/mole, and 192 ± 5 kJ/mol for CO_2/CO ratios of 0.61, 1.13, and 2.42, respectively. These activation energies are equal within the uncertainty, and so, it can be stated that that activation energy of the reaction is independent of the oxygen partial pressure (*i.e.*, the CO_2/CO ratio) within the wüstite phase field. The reason for the greater deviation for the activation energy for the CO_2/CO ratio of 1.13 is likely because this was obtained from the experiments using carbon 14, which were generally less precise than the carbon-13 experiments, particularly at the lower CO_2/CO ratios. Turkdogan and Vinters[51] compiled data from various researchers and found the activation energy to be 192 kJ/mol for the dissociation of carbon dioxide on the surface of wüstite when a CO_2/CO ratio of 1 was used. This value agrees with the values obtained from the experimental data from this study. Similarly, a value of 193 kJ/mol was found for liquid slags,[50] which is also consistent with the value found from this study. However, Grabke[10] obtained a value of 143 kJ/mole with a ratio of CO_2/CO equal to 1, using the isotope exchange technique. This is in contradiction of the value obtained from this study and that of Turkdogan and Vinters.

Over the relatively limited oxygen potential range, a single straight line can describe all magnetite data at a given temperature. Only two temperatures were considered for magnetite, both of which produced essentially the same slope (*i.e.*, slope equals 1). By using Eqs. [30] and [31], the change in the rate constant from 1123 K (850 °C) to 1268 K (995 °C) was found to be consistent with the reaction on magnetite having an activation energy of 181 kJ/mol. This is consistent with the activation energies found for the reaction on wüstite.

B. CO_2 Dissociation on Magnetite

Work was done in the magnetite region using carbon 14 at a temperature of 1268 K (995 °C) and using carbon 13 at temperatures of 1123 K (850 °C) and 1268 K (995 °C). At 1268 K (995 °C), the data using carbon 14 gave a slope of –0.9 (Eq. [28]) and using carbon 13 gave a slope of –1.0 (Eq. [31]) on graphs of the apparent rate constant *vs* the CO_2/CO ratio. At 1123 K (850 °C), using carbon 13, the data gave a slope of –1.0 (Eq. [30]). It can be seen from this that the carbon-14 and carbon-13 values at 1268 K (995 °C) are in agreement. The carbon-13 data are less scattered than the carbon-14 data and so seems more reliable. The slopes of the lines of the carbon-13 data do not compare well with the values that Grabke[10] obtained. Grabke found slopes of –0.5 for temperatures of 1073 K (800 °C), 1173 K (900 °C), and 1256 K (983 °C). The authors offer no explanation for this discrepancy. The experiments done in this study for the magnetite phase field all were conducted in the oxygen partial pressure range, where the oxide would have a metal excess. This means that the predominant defects were interstitial iron ions.[52] According to Dieckmann,[53] because the stoichiometry of magnetite does not vary much in this region, the concentration of free electrons is buffered by Eq. [32], which is expressed as follows.

$$Fe^{2+} \rightleftarrows Fe^{3+} + e' \qquad [32]$$

The apparent rate constant is given by Eq. [33] as follows:

$$k_a = k_o a_O^{-m} \qquad [33]$$

Grabke and Viefhaus[8] have stated that the oxygen activity dependence can result from either adsorbed oxygen or the electronic or ionic disorder of the oxide. The first of these two influences does not seem to be feasible, as it was found for wüstite that adsorbed oxygen was not a factor above 1173 K (800 °C).[8] Because this was the case for wüstite, it seems unlikely that adsorbed oxygen would influence the kinetics in magnetite for the temperatures studied. This means that the second influence must occur. Therefore, the oxygen activity dependence must be from the electronic disorder of magnetite. In magnetite, a redox equilibrium exists given by Eq. [32]. Therefore, if Eq. [33] is taken into account along with Eq. [34], which gives the surface reaction of the dissociation of carbon dioxide, it is found that the proportionality given by Eq. [35] is true. Equations [34] and [35] are as follows:

$$CO_2 + 2e' \rightleftarrows CO + O^{2-} \qquad [34]$$

$$\left(\frac{Fe^{3+}}{Fe^{2+}}\right)^2 \propto \left(\frac{P_{CO_2}}{P_{CO}}\right) \qquad [35]$$

From this, it is evident that the m parameter, given in Eq. [33], has a value of 1 if the electron concentration is controlled by the previous equations. Therefore, the data obtained in this study is consistent with the transfer of two electrons to the adsorbed gas (*i.e.*, $CO^-_{2(ads)} \rightleftarrows O^{2-}_{(ads)} + CO + h^\bullet$).

C. CO_2 Dissociation on the Surface of Wüstite

In this range it can be seen that one straight line does not accurately describe the data. At 1268 K (995 °C) (Figure 6), the data can be broken into three regions. The one closest to the iron–wüstite border is given by Eq. [36]. The middle line is given by Eq. [37] and the one closest to the wüstite–magnetite border is given by Eq. [38]. Equations [36] through [38] are expressed as follows:

$$\text{Log}\,(k_a) = -0.51(\pm 0.05)\text{Log}\left(\frac{CO_2}{CO}\right) - 7.19(\pm 0.01) \qquad [36]$$

$$\text{Log}\,(k_a) = -0.66(\pm 0.03)\text{Log}\left(\frac{CO_2}{CO}\right) - 7.21(\pm 0.01) \qquad [37]$$

$$\text{Log}\,(k_a) = -1.03(\pm 0.05)\text{Log}\left(\frac{CO_2}{CO}\right) - 7.09(\pm 0.03) \qquad [38]$$

The changes in the slopes of the lines occur at CO_2/CO ratios of 0.68 and 2.17. These values were obtained by determining the CO_2/CO ratios at which the lines crossed (*i.e.*, where the rate constants were equal).

At a temperature of 1123 K (850 °C), one straight line, again, does not accurately describe the data. From Figure 5, it can be seen that the data is described better by two straight lines, which are given in the following Eqs. [39] and [40]:

$$\text{Log}\,(k_a) = -0.59(\pm 0.03)\text{Log}\left(\frac{CO_2}{CO}\right) - 8.06(\pm 0.01) \qquad [39]$$

$$\text{Log}\,(k_a) = -1.01(\pm 0.05)\text{Log}\left(\frac{CO_2}{CO}\right) - 8.10(\pm 0.01) \qquad [40]$$

The point at which the slopes of the lines change occurs at a CO_2/CO ratio of 1.21. This value was obtained by averaging the highest CO_2/CO ratio for the first line and the lowest CO_2/CO ratio for the second line. This was done because no data was obtained that enabled the exact location of the boundary to be determined.

The previous results in the wüstite region, at a first glance, seem to be in contradiction with other studies that have been conducted.[10,38] Table II shows the slopes of the lines found in each of these studies at various temperatures. From this table, it can be seen that, for Grabke's[10] work, the slope increased as the

Table II. Values of the Slopes of the Lines in the Wüstite Region

Temperature (K (°C))	Negative Values of the Slopes				
	This Study				
	w_1	w_2	w_3	Grabke[10]	Meschter and Grabke[38]
1073 (800)				1.0	0.52
1123 (850)	0.59	0.59	1.01		
1173 (900)				0.7	0.68
1256 (983)				0.6	
1268 (995)	0.51	0.66	1.03		
1273 (1000)					0.59

For temperatures below 1184 K (911 °C) the phases are actually w_1', w_2', and w_3'

Table III. Estimated O/Fe Values for the Changes in Slopes from the Data of this Study for the Wüstite Region and for the Pseudo Phase Boundaries Proposed by Vallet and Carel[54]

Temperature (K (°C))	O/Fe Values at Breaks in Curves	Vallet and Carel[54]	
		Boundary	O/Fe Value
1123 (850)	none found	w_1'/w_2'	1.078
	1.091 ± 0.017	w_2'/w_3'	1.090
1268 (995)	1.075 ± 0.022	w_1/w_2	1.078
	1.112 ± 0.016	w_2/w_3	1.114

temperature decreased, but with Meschter and Grabke's[38] work, the slope increased and then decreased with temperature. However, it can be seen that the slopes from this study encompass all values for the slopes found by the other researchers. The authors offer no explanation for this discrepancy except to point out that the present work is based on a significantly larger data set, which may have revealed features previously missed.

The changes in the slopes that occurred in the wüstite phase field correspond almost exactly to the pseudo phase boundaries proposed by Vallet and Carel.[54] This is shown in Table III.

The results obtained for the wüstite region show that the simple picture proposed by Grabke[10] does not accurately describe the kinetics in this phase field. Grabke and Viefhaus[8] used a simple defect structure to explain the results they achieved in the wüstite phase field, as their data seemed to fit a single straight line. However, a simple defect structure does not occur in wüstite, and so, the kinetics of the system should not be explained through the use of such a defect structure. This study shows that one straight line cannot explain the kinetics in this phase field, and instead, up to three lines are needed to model the data.

D. *Pseudo Phases of Wüstite*

From this study, it can be seen that the kinetics of the oxygen exchange reaction on wüstite are not as simple as originally thought. It has been shown that the rate

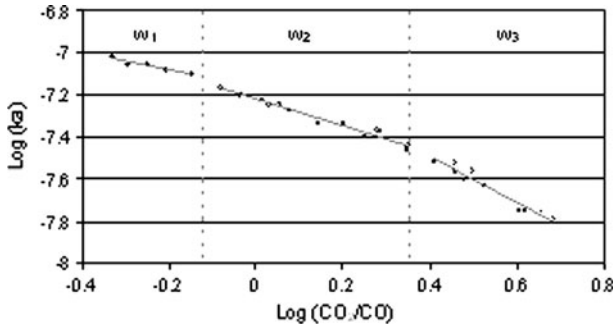

Fig. 8—The effect of the oxygen partial pressure on the apparent rate constant at a temperature of 1268 K (995 °C) in the wüstite phase field. The dotted lines represent the boundaries between the three pseudo phases w_1, w_2, and w_3 given by Vallet and Carel.[54]

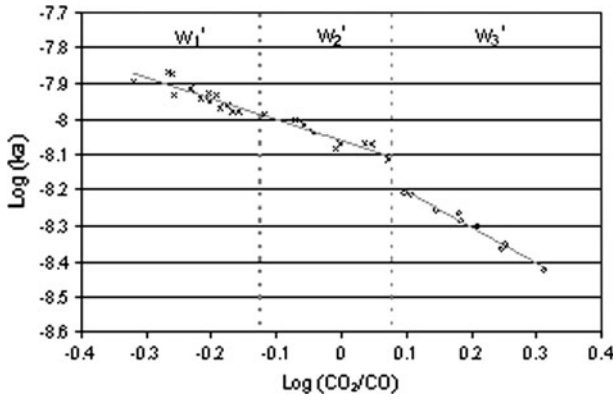

Fig. 9—The effect of the oxygen partial pressure on the apparent rate constant at a temperature of 1123 K (850 °C) in the wüstite phase field. The dotted lines represent the boundaries between the three pseudo phases w_1', w_2', and w_3' given by Vallet and Carel.[54]

constant for this reaction cannot be represented by one straight line at the temperatures considered. The results have provided evidence for the existence of three straight lines at 1268 K (995 °C) (Figure 8) and two at 1123 K (850 °C) (Figure 9). These regions can be related to the pseudo phases in the wüstite phase field initially proposed by Vallet and Raccah[18] and by Kleman.[19] The boundaries of the pseudo phases were refined by Vallet and Carel,[53] and the boundary between w_1/w_2 phases and w_2/w_3 phases were given by CO_2/CO ratios of 0.75 and 2.26, respectively, at 1268 K (995 °C). At 1123 K (850 °C) the boundaries between the w_1'/w_2' and w_2'/w_3' phases are given by the CO_2/CO ratios of 0.75 and 1.19, respectively. Figures 8 and 9 show that the proposed pseudo phases agree well with the breaks in the kinetic data at 1268 K (995 °C), but for the 1123 K (850 °C) data, only two regions were found. The point at which there is a change in the slope of the 1123 K (850 °C) data corresponds to the boundary between the w_2' and w_3' pseudo phases proposed by Vallet and Carel.[54] However, there does not seem to be a change in slope where the boundary between the w_1' and w_2' pseudo phases was proposed. This could be because

Table IV. Estimated O/Fe Values for the Changes in Slopes of Kinetic Data (this Study), the Changes in Slopes of Electrical Conductivity Data,[29] and the Pseudo Phase Boundaries[54]

	Estimation of the O/Fe Values at Breaks in Curves		Vallet and Carel[54]	
Temperature (K (°C))	This study	Geiger *et al.*[29]	Boundary	O/Fe
1333 (1060)		1.08	w_1/w_2	1.081
1273 (1000)		1.07	w_1/w_2	1.078
		1.11	w_2/w_3	1.117
1268 (995)	1.075 ± 0.022		w_1/w_2	1.078
	1.112 ± 0.016		w_2/w_3	1.114
1173 (900)		none found	w_1'/w_2'	1.079
		1.09	w_2'/w_3'	1.091
1123 (850)	none found	none found	w_1'/w_2'	1.078
	1.091 ± 0.017	1.09	w_2'/w_3'	1.090

there is more scatter in the 1123 K (850 °C) data in what should be the w_1' and w_2' pseudo phases. In the 1268 K (995 °C) data, the slopes for the w_1 and w_2 pseudo phases are –0.51 and –0.66, respectively. It is possible that the scatter found in the 1123 K (850 °C) data could obscure a change in slope between the w_1' and w_2' pseudo phases. Therefore, this data provides good evidence to support the existence of three pseudo phases in wüstite at 1268 K (995 °C) and at least two at 1123 K (850 °C). The existence of these pseudo phases has been the subject of much discussion in the past, and it is still up for debate whether they exist.[33,36,55,56]

Geiger *et al.*[29] made electrical conductivity measurements in the wüstite phase field at temperatures of 1123 K (850 °C), 1273 K (1000 °C), and 1333 K (1060 °C). They found changes in the slopes of their data in graphs of the log of the electrical conductivity *vs* the log of the oxygen partial pressure. The oxygen partial pressures at which these changes in slopes occur correspond well with those obtained in this study. Table IV shows the values of the slope changes found by Geiger *et al.*,[29] those obtained from this work, and the pseudo phase boundaries proposed by Vallet and Carel.[54]

From Table IV, it can be seen that the changes in the slopes of the conductivity curves agree with the changes in the slopes of the kinetic data from this study. It also shows that the change in slopes correspond with the pseudo phase transitions. However, neither the conductivity study nor this study found a slope change corresponding to the proposed boundary between the w_1' and w_2' pseudo phases.

The conductivity data[29] supports the results obtained from this study that there are three distinct regions in the wüstite phase at 1268 K (995 °C) but only two at 1123 K (850 °C). From this analysis, it can be hypothesized that there are only two pseudo phase regions at 1123 K (850 °C) in wüstite instead of the three proposed by Vallet and Carel,[54] or that there are three pseudo phases at 1123 K (850 °C) but that the electron defect dependency on the partial pressure of oxygen does not change between w_1' and w_2'.

V. CONCLUSIONS

The aim of this work was to investigate the oxygen exchange reaction ($CO_2 \rightleftarrows CO + \frac{1}{2}O_2$) on iron, wüstite, and magnetite. This was done by measuring the kinetics of the reaction using an isotope exchange technique. The conclusions obtained from this study are as follows:

1. It was found that the activation energy in the wüstite phase was 192 ± 3 kJ/mol, 180 ± 14 kJ/mol, and 192 ± 5 kJ/mol for CO_2/CO ratios of 0.61, 1.13, and 2.42, respectively. Therefore, it was concluded that the activation energy is independent of the oxygen partial pressure in the wüstite phase field.
2. The data obtained in the iron region gives evidence to support the conclusion that the rate constant was independent of the oxygen partial pressure at 1123 K (850 °C). The rate constant found at 1123 K (850 °C) is given by Eq. [29].
3. In the magnetite region, it was found that the rate constant was inversely dependent on the oxygen partial pressure in the metal excess stoichiometry range of the oxide. This is consistent with the transfer of two electrons to the adsorbed gas (*i.e.*, $CO^-_{2(ads)} \rightleftarrows O^{2-}_{(ads)} + CO + h^\bullet$). Equations [30] and [31] give the rate constants obtained for temperatures of 1123 K (850 °C) and 1268 K (995 °C), respectively.
4. In the wüstite phase field, the situation has been found to be more complicated than in either of the other fields studied. In this region, the oxygen exchange reaction was investigated at temperatures of 1123 K (850 °C) and 1268 K (995 °C). It was found at the lower temperature that a change of slope in the data occurred at a CO_2/CO ratio of 1.21 and that the data was best described by two straight lines. Equations [39] and [40] give the rate constants obtained for the two pseudo phase regions (w_1' and w_3'). The first of which is for the data near the iron–wüstite boundary, and the second is for the data near the wüstite–magnetite boundary.

   At the higher temperature, there were found to be slope changes at CO_2/CO ratios of 0.68 and 2.17. These break points correspond exactly with the proposed pseudo phase boundaries at this temperature, suggesting that the kinetics are influenced by the defect structure of the pseudo phase. Equations [36] through [38] are for the rate constants for the three lines going across the phase field from the iron-rich to the oxygen-rich side (*i.e.*, w_1, w_2, and w_3).

ACKNOWLEDGMENTS

The authors are indebted to Dr. J. S. Kirkaldy for his support of this project through most of the early stages. The authors are also grateful for the financial support of the Natural Science and Engineering Research Council of Canada.

REFERENCES

1. Y. Sasaki and G.R. Belton: *Metall. Trans. B*, 1980, vol. 11B, pp. 221–24.
2. Y. Sasaki and G.R. Belton: *Metall. Trans. B*, 1983, vol. 14B, pp. 267–72.
3. M.H. LaBranch and G.J. Yurek: *Oxid. Met*., 1987, vol. 28, pp. 73–98.
4. X.G. Zheng and D.J. Young: *Corros. Sci*., 1994, vol. 36, pp. 1999–2015.
5. P.C. Glaws and G.R. Belton: *Metall. Trans. B*, 1990, vol. 21B, pp. 511–19.
6. X.G. Zheng and D.J. Young: *Corros. Sci*., 1996, vol. 38, pp. 1877–97.
7. X.G. Zheng and D.J. Young: *Mater. Sci. Forum*, 1997, vols. 251–254, pp. 567–74.
8. H.J. Grabke and H. Viefhaus: *Ber. Bunsenges. Phys. Chem*., 1980, vol. 84, pp. 152–59.
9. H.J. Grabke: *Ann. NY Acad. Sci*., 1973, vol. 213, pp. 110–36.
10. H.J. Grabke: *Ber. Bunsenges. Phys. Chem*., 1965, vol. 69, p. 48.
11. P. Vallet, M. Kleman, and P. Raccah: *C.R. Hebd. Acad. Sci. Paris*, 1963, vol. 256, p. 136.
12. C. Carel and P. Vallet: *C.R. Hebd. Acad. Sci. Paris*, 1964, vol. 258, p. 3281.
13. P. Vallet and C. Carel: *Ann. Chim*., 1970, vol. 5, pp. 246–49.
14. C. Carel and J.R. Gavarri: *Mater. Res. Bull*., 1976, vol. 11, pp. 745–56.
15. C. Carel, D. Weigel, and P. Vallet: *C.R. Hebd. Acad. Sci. Paris*, 1964, vol. 258, p. 6126.
16. C. Carel, D. Weigel, and P. Vallet: *C.R. Hebd. Acad. Sci. Paris*, 1965, vol. 260, p. 4325.
17. P. Vallet and P. Raccah: *C.R. Hebd. Acad. Sci. Paris*, 1964, vol. 258, p. 3679.
18. P. Vallet and P. Raccah: *Mem. Sci. Rev. Met*., 1965, vol. 62, pp. 1–29.
19. M. Kleman: *Mem. Sci. Rev. Met*., 1965, vol. 62, p. 457.
20. C. Carel: *C.R. Hebd. Acad. Sci. Paris C*, 1967, vol. 265, p. 533.
21. C. Picard and M. Dodé: *Bull. Soc. Chim. France*, 1970, vol. 7, p. 2486.
22. P. Vallet: *C.R. Hebd. Acad. Sci. Paris C*, 1975, vol. 281, pp. 291–94.
23. P. Vallet and C. Carel: *Rev. Chim. Miner*., 1986, vol. 23, p. 709.
24. E. Takayama and N. Kimizuka: *J. Electrochem. Soc*., 1980, vol. 127, pp. 970–79.
25. O.T. Sørensen: *Nonstoichiometric Oxides*, Academic Press, New York, NY, 1981.
26. J.R. Gavarri, C. Carel, and D. Weigel: *J. Solid State Chem*., 1979, vol. 29, pp. 81–95.
27. B.E.F. Fender and F.D. Riley: *J. Phys. Chem. Solids*, 1969, vol. 30, pp. 793–98.
28. H.F. Rizzo, R.S. Gordon, and I.B. Cutler: *J. Electrochem. Soc*., 1969, vol. 116, pp. 266–74.
29. G.H. Geiger, R.L. Levin, and J.B. Wagner, Jr.: *J. Phys. Chem. Solids*, 1966, vol. 27, p. 947.
30. J. Molenda, A. Stoklosa, and W. Znamirowski: *Phys. Status Solidi B*, 1987, vol. 142, pp. 517–29.
31. B. Swaroop and J.B. Wagner, Jr.: *Trans. AIME*, 1967, vol. 239, pp. 1215–18.
32. F.E. Rizzo and J.V. Smith: *J. Phys. Chem*., 1968, vol. 72, p. 485.
33. R.A. Giddings and R.S. Gordon: *J. Am. Ceram. Soc*., 1973, vol. 56, pp. 111–16.
34. R.A. Giddings and R.S. Gordon: *J. Electrochem. Soc*., 1974, vol. 121, pp. 793–800.
35. M. Hayakawa, J.B. Cohen, and T.B. Reed: *J. Am. Ceram. Soc*., 1972, vol. 55, pp. 160–64.
36. J. Nowotny and I. Sikora: *J. Electrochem. Soc*., 1978, vol. 125, pp. 781–86.
37. H.J. Grabke, K.J. Best, and A. Gala: *Werkst. Korros*., 1970, vol. 21, pp. 911–16.
38. P.J. Meschter and H.J. Grabke: *Metall. Trans. B*, 1979, vol. 10B, pp. 323–29.
39. H.J. Grabke: *Proc. 3rd Int. Congress on Catalysis*. North Holland Publishing Company, Amsterdam, The Netherlands, 1964, p. 928.
40. H.J. Grabke: *Ber. Bunsenges. Phys. Chem*., 1967, vol. 71, p. 1067.
41. A.W. Cramb, W.R. Graham, and G. R. Belton: *Metall. Trans. B*, 1978, vol. 9B, pp. 623–29.
42. A.W. Cramb and G.R. Belton: *Metall. Trans. B*, 1981, vol. 12B, pp. 699–704.
43. A.W. Cramb and G.R. Belton: *Metall. Trans. B*, 1984, vol. 15B, pp. 655–61.
44. Y. Sasaki, S. Hara, D.R. Gaskell, and G.R. Belton: *Metall. Trans. B*, 1984, vol. 15B, pp. 563–71.
45. S.K. El-Rahaiby, Y. Sasaki, D.R. Gaskell, and G.R. Belton: *Metall. Trans. B*, 1986, vol. 17B, pp. 307–16.
46. S. Sun, Y. Sasaki, and G.R. Belton: *Metall. Trans. B*, 1988, vol. 19B, pp. 959–65.
47. M. Mori, K. Morita, and N. Sano: *ISIJ Int*., 1996, vol. 36, pp. 624–30.
48. J.E. Bauer, P.M. Williams, and E.T.M. Druffel: *Anal. Chem*., 1992, vol. 64, pp. 824–27.
49. E. Worral: Ph.D. Dissertation, McMaster University, Hamilton, Canada, 2005.
50. M. Barati and K.S. Coley: *Metall. Mater. Trans. B*, 2005, vol. 36B, pp. 169–78.
51. E.T. Turkdogan and J.V. Vinters: *Metall. Trans*., 1972, vol. 3, p. 1561.
52. R. Dieckmann and H. Schmalzried: *Ber. Bunsenges. Phys. Chem*., 1977, vol. 81, pp. 344–47.
53. R. Dieckmann: *J. Phys. Chem. Solids*, 1998, vol. 59, pp. 507–25.
54. P. Vallet and C. Carel: *Mater. Res. Bul*., 1979, vol. 14, pp. 1181–94.
55. C. Gleitzer: *Key Eng. Mater*., 1997, vols. 125–6, pp. 355–417.
56. R.M. Hazen and R. Jeanloz: *Rev. Geophys. Space Phys*., 1984, vol. 22, pp. 37–46.